

SimTrans: A Self-supervised Method for Biomedical Image Segmentation

Shengfan Wang
CSBIO
SEIEE 2-306

diofan0814@sjtu.edu.cn

Zhen Zhou
CSBIO
SEIEE 2-306

zz20020101@sjtu.edu.cn

Jiabei Cheng
CSBIO
SEIEE 2-306

jiabei_cheng@sjtu.edu.cn

Changyong Li
CSBIO
SEIEE 2-306

steven_li@sjtu.edu.cn

Abstract

Due to privacy concerns and the high cost of annotation, biomedical image datasets are small and labeled samples are scarce. Existing convolutional neural network (CNN)-based segmentation models suffer from limited receptive fields, which restrict their ability to capture global features, leading to a decrease in accuracy. To address these issues, we propose a deep learning network called SimTrans, which is based on self-supervised learning. The SimTrans method initially trains data using the self-supervised framework SimCLR, overcoming the limitations of data scarcity by directly capturing the distributional features of the data without relying on labels. Subsequently, we separate the encoder part of SimCLR and combine it with the Transformer framework, adding a decoder to accomplish an end-to-end segmentation task. This approach combines the advantages of SimCLR and the Transformer framework. The paper begins by introducing the self-supervised learning framework SimCLR and the Swin Transformer framework. It then describes the weighted structured loss function used in the downstream task. Next, the proposed SimTrans deep learning framework is presented in detail, followed by experimental evaluations that include experimental settings, results, and analysis. SimTrans provides an innovative solution to address the limitations of small biomedical image datasets, scarcity of labeled samples, and the challenges of capturing global features in CNN-based segmentation models. By combining self-supervised learning and the Transformer framework, SimTrans effectively extracts global features and improves segmentation accuracy.

1. Introduction

With the rapid development of deep learning technology, many fields have started to adopt deep learning techniques to improve task efficiency. Training deep

learning models requires a large amount of data, and this data needs to have corresponding labels in order to train models that have strong fitting and generalization capabilities. However, in the field of biomedical imaging, it is not possible to obtain a large amount of data due to patient privacy concerns. Additionally, the annotation of biomedical images requires professional medical experts, which further increases the cost of data annotation. As a result, there is a scarcity of biomedical imaging datasets, and the number of annotated data samples is even smaller. Biomedical image segmentation typically involves pixel-level classification of lesions, tissues, and organs in biomedical images. These lesions, tissues, and organs generally occupy a large space or are far apart in biomedical images. Based on this characteristic, we analyzed the current mainstream biomedical image segmentation models based on convolutional neural networks (CNNs). These models use traditional convolutional approaches for feature extraction. However, traditional convolutions are limited by their receptive field and can only extract local features of the target, failing to capture global features. This can cause the model to struggle in distinguishing background regions in the image and may misclassify background pixels as the features of interest, leading to a decrease in segmentation accuracy. Researchers have proposed various methods to address these issues, such as using multiple convolutional kernels of different sizes or downsampling to reduce image resolution. These methods partially solve the problem of CNNs' inability to capture global features. However, they either increase the model's complexity and reduce its runtime speed or sacrifice some local feature information, resulting in a decrease in model accuracy without achieving a balance. To address the aforementioned problems, this paper proposes an end-to-end deep learning network based on self-supervised learning. In this approach, the self-supervised framework SimCLR is first employed for training, overcoming the lack of labeled data by directly extracting the

data distribution features. Then, the encoder part of SimCLR, which captures the data distribution, is separated and combined with a decoder to accomplish the downstream end-to-end segmentation task. This method is named SimTrans, derived from the combination of the self-supervised framework SimCLR and the Transformer framework. The paper begins by introducing the self-supervised learning framework SimCLR, followed by an introduction to the Swin Transformer framework. It then presents the weighted structured loss function used for the downstream task and introduces the proposed SimTrans deep learning framework. Finally, the paper conducts experiments to evaluate the proposed model, providing details on the experimental setup, results, and analysis.

2. Related Work

2.1. SimCLR

To address the scarcity of biomedical image datasets, researchers aim to develop models that can learn features directly from the data without the need for labeled data. This approach, known as self-supervised learning, allows models to learn features from the data itself. One widely studied self-supervised learning framework in the field is SimCLR [1], proposed by Hinton et al. SimCLR consists of four main components: data augmentation, a base encoder, a projection head, and a contrastive loss. The framework is designed to learn powerful representations from unlabeled data. In SimCLR, data augmentation is applied to generate multiple augmented versions of each unlabeled sample. These augmented samples are then passed through the base encoder, which extracts their features. The projection head further processes the encoded features to produce informative representations. Finally, the contrastive loss function encourages similar representations of augmented samples from the same sample while pushing representations from different samples apart.

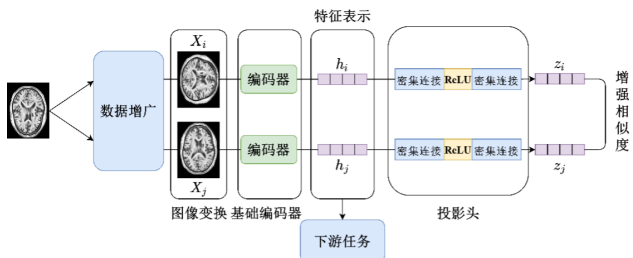


Figure 1. Framwork of SimCLR.

The overall objective of SimCLR is to maximize agreement between differently augmented views of the

same data sample while minimizing agreement between different samples. This enables the model to learn rich and discriminative representations without the need for explicit labels. SimCLR has garnered significant attention from researchers and has achieved remarkable results in various computer vision tasks, including biomedical image analysis.

The data augmentation module in SimCLR performs random transformations on given data samples to generate two correlated views of the same sample, denoted as x_i and x_j . These two views are treated as a positive sample pair. Data augmentation techniques used in SimCLR include random cropping, resizing, color distortion, and Gaussian blur. These operations generate pseudo-labels, which are then utilized to train the model. The encoder in SimCLR extracts feature vectors, represented as h_i and h_j , from the augmented data samples. The choice of encoder is not constrained and commonly used backbone frameworks like VGG and ResNet can serve as encoders in SimCLR. The projection head maps the data representations to the space of contrastive loss. A common approach is to use a single-layer multilayer perceptron (MLP) for this mapping, as shown in Equation (1):

$$z_i = g(h_i) = W^{(2)}\sigma\left(W^{(2)}h_i\right) \quad (1)$$

Here, $g(\cdot)$ represents the mapping function, σ is the ReLU activation function. According to the experimental analysis by the authors of SimCLR, defining the contrastive loss on the projected feature representation z_i tends to yield better results compared to using the feature representation h_i directly from the encoder. The contrastive loss module defines the contrastive loss function for the contrastive prediction task. The key component of SimCLR is the normalized temperature-scaled cross-entropy loss (NT-Xent) used as the contrastive loss, given by Equation (2):

$$\ell_{i,j} = -\log \frac{\exp(\text{sim}(z_i, z_j) / \tau)}{\sum_{k=1}^{2N} \mathbb{1}_{[k \neq i]} \exp(\text{sim}(z_i, z_k) / \tau)} \quad (2)$$

First, it calculates the similarity between a positive pair and all negative representations. The cosine similarity function is commonly used as a distance metric. Then, negative cross-entropy loss is employed to calculate the loss function for the positive sample pair (i, j) .

2.2. Swin Transformer

Swin Transformer [4] is a hierarchical structure that builds feature maps by merging image patches at deeper layers, allowing flexible modeling at multiple scales. It achieves a linear computational complexity

relative to the image size by computing self-attention within each local non-overlapping window. Additionally, Swin Transformer enables cross-window connections, as shown in Figure 2. The self-attention computation of a new window spans the boundaries of previously processed windows in layer l , providing cross-window connections between adjacent non-overlapping windows. This operation has been found effective in tasks such as image classification, object detection, and semantic segmentation. The ability to model visual entities of various scales and replace quadratic complexity with linear computational complexity contributes to Swin Transformer’s versatility as a backbone for various visual tasks.

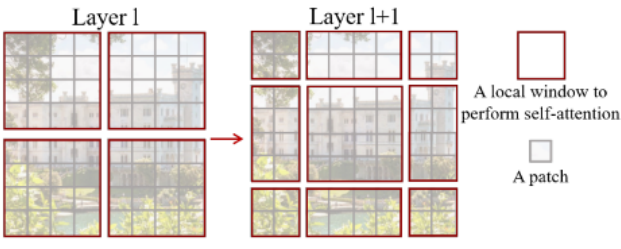


Figure 2. Self-attention computation for non-overlapping windows.

Swin Transformer consists of a Multi-head Self-Attention module (MSA) based on movable windows, followed by a two-layer Multilayer Perceptron (MLP) with Gaussian Error Linear Units (GELU) as the non-linear activation function. GELU is a high-performance neural network activation function that weights the inputs rather than gating them with signs as in ReLU. Layer Normalization (LN) is applied before each MSA module and each MLP, and a residual connection is employed after each module, as shown in Figure 3. The computational complexity of the standalone MSA module in Swin Transformer has a quadratic relationship with the image size, as shown in Equation (3):

$$\Omega(MSA) = 4hwC^2 + 2(hw)^2C \quad (3)$$

However, in Swin Transformer, the self-attention computation is performed within non-overlapping local windows, resulting in a linear computational complexity relative to the image size, as shown in Equation (4):

$$\Omega(W - MSA) = 4hwC^2 + 2M^2hwC \quad (4)$$

Here, M is a constant. Furthermore, Swin Transformer incorporates relative position information into the attention computation, as shown in Equation (5):

$$\text{Attention}(Q, K, V) = \text{SoftMax} \left(\frac{QK^T}{\sqrt{d}} + B \right) V \quad (5)$$

Where Q , K , and V represent the query matrix, key matrix, and value matrix, respectively. d is the dimension, and B represents the relative position bias. Compared to using absolute positions, incorporating relative positional biases significantly improves the model’s performance. Additionally, Swin Transformer introduces inductive biases such as locality, hierarchical feature representation, and translation equivariance, enabling it to serve as a universal backbone network for various image recognition tasks.

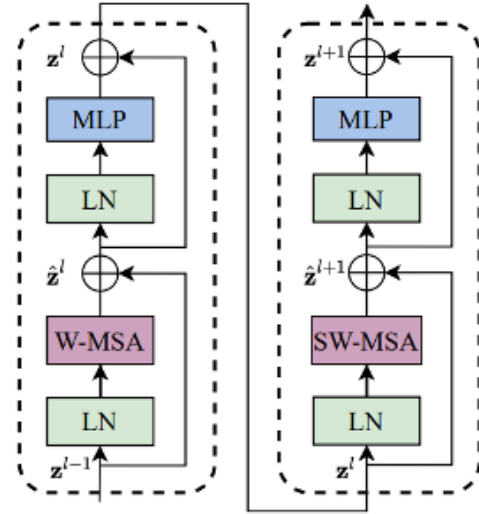


Figure 3. Block of Swin Transformer.

2.3. Residual Channel Attention

The Residual Channel Attention (RCA) [6] module combines channel attention and residual connections. By using channel attention, it can capture features from different channels and enhance channel-wise information. The residual connections then connect the features, allowing for more refined feature representation. The structure of the RCA module is illustrated in Figure 5.

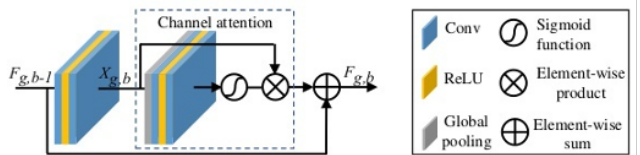


Figure 4. Structure of RCBA.

2.4. Multi-scale Dilated Convolution

Multi-scale dilated convolution [5] is composed of convolutions with different dilation rates. Firstly, the feature map undergoes multiple convolution layers with different dilation rates. Then, the output results from each convolution layer are cascaded together to form the output of the entire module. This approach not only addresses the issue of information discontinuity caused by dilation but also helps the model capture multi-scale feature information. Figure 6 illustrates dilated convolutions, with the left side showing a dilated convolution with a dilation rate of 2, and the right side showing a dilated convolution with a dilation rate of 3.

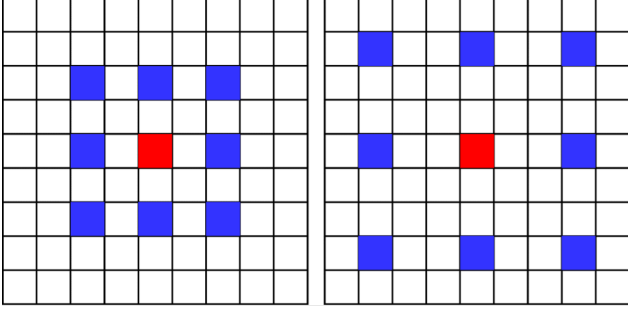


Figure 5. Structure of MSD.

3. Method

We utilize Swin Transformer as the encoder in the SimCLR framework and train it using unlabeled data, allowing the Swin Transformer to learn the distribution and features of the data with the help of pseudo-labels. Then, we apply the learned feature encoder to downstream segmentation tasks. Based on SimCLR and Swin Transformer, we design a deep learning network model called SimTrans, as shown in Figure 4. In the downstream tasks, to achieve an end-to-end output, a simple decoder is employed. It fuses the features obtained at different stages of the Swin Transformer and includes a decoder module that upsamples the fused features for comparison with the label map. Additionally, to better train the model, we propose a weighted structured loss function based on existing loss functions. It is a weighted sum of binary cross-entropy loss (BCE) and intersection over union loss (IOU):

$$L(s, y) = w * L_{bce}(s, y) + L_{iou}(s, y) \quad (6)$$

Here, Y represents the label, W represents the edge weight $w = 1 + 5 * |(ap(x) - y)|$, $ap(\cdot)$ represents the average pooling operation.

The SimTrans model is based on the self-supervised learning framework SimCLR and the Transformer

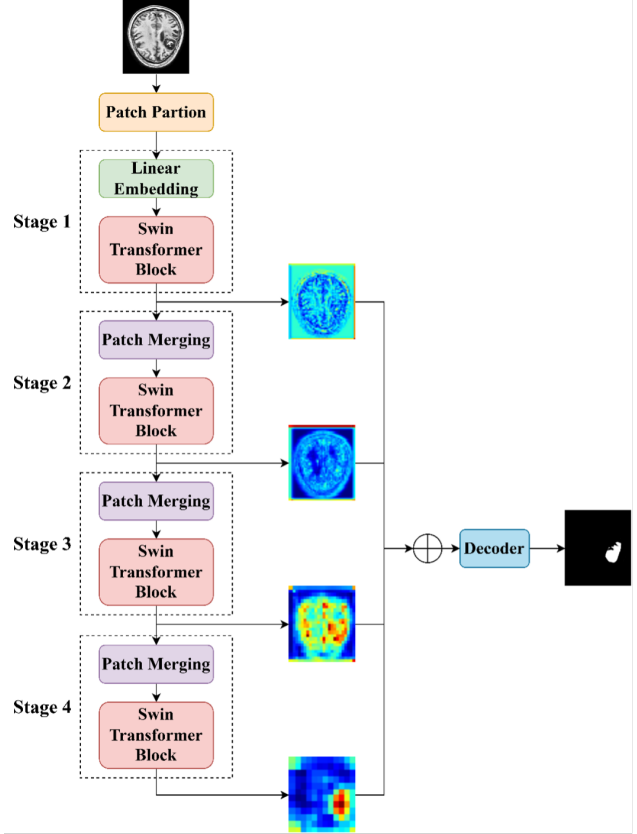


Figure 6. Structure of SimTrans.

model, specifically designed for the challenges of biomedical image datasets with limited annotated data. This model leverages the strategy of SimCLR, which involves data augmentation techniques to generate multiple augmented images from a single image. These generated images serve as positive examples, while the other images in a training batch act as negative examples. This allows for the reduction of the distance between positive examples and the separation of negative examples. After deciding to use the self-supervised learning framework of SimCLR, we compared various commonly used backbone architectures such as VGG and ResNet. However, these architectures, based on traditional convolutional neural networks, have certain limitations, such as fixed receptive fields and large model sizes. Considering the need for global feature consideration in biomedical images, a model capable of capturing long-range dependencies was preferred. Therefore, the Transformer framework was considered, and different Transformer architectures such as ViT and TransUNet were evaluated. Ultimately, Swin Transformer was selected due to its ability to capture global features using the Trans-

former’s long-range dependency modeling capabilities. Additionally, the introduction of a sliding window approach for attention computation in Swin Transformer reduced the number of parameters required for global attention computation. Moreover, Swin Transformer has a hierarchical design that continuously reduces the resolution of input feature maps, similar to the down-sampling process in convolutional neural networks, to expand the receptive field. Using Swin Transformer as the encoder part of SimCLR, training is conducted using generated pseudo-labels. Once training is completed, for the downstream task of biomedical image segmentation, a decoder is added to Swin Transformer. The decoder consists of two modules: Residual Channel Attention Block (RCAB) and Multi-Scale Dilated Convolution (MSD).

4. Experiment

This study conducted experimental validation of the proposed deep learning model on the ATLAS (Automatic Labeling of Brain Stroke Lesion) dataset [3], which is a publicly available dataset for brain stroke lesion segmentation. The dataset consists of a total of 229 T1-weighted brain magnetic resonance imaging (MRI) images provided by 11 different medical research centers. These images are expertly annotated by professional physicians. Each three-dimensional image has a voxel size of $0.9\text{mm} \times 0.9\text{mm} \times 0.3\text{mm}$ and contains 189 slices. Each slice has dimensions of 233×197 . The entire ATLAS dataset consists of 43,281 two-dimensional slices. In this study, 10,203 labeled data were processed and used for validation in the downstream segmentation task, while the remaining 33,078 slices were used for self-supervised learning to learn the features of brain stroke data. Three evaluation metrics, namely Dice coefficient, mean intersection over union (IoU), and precision, were selected to quantify the performance of the proposed model. All the experiments were conducted in the PyTorch framework and trained using Nvidia-RTX 3090Ti GPUs. The deep learning models were trained for a total of 50 epochs.

4.1. Results and Analysis

This study employed the self-supervised learning framework SimCLR to learn the features of unlabeled data. SimCLR utilizes data augmentation techniques to generate pseudo-labels, as shown in Figure 7.

To assess whether the SimTrans model focuses more on the lesion regions at different stages, the feature maps were visualized and analyzed. Figure 8 illustrates the visualization of the feature maps.

Figure 8 displays the following images from left to right: the original brain MRI image, feature maps from

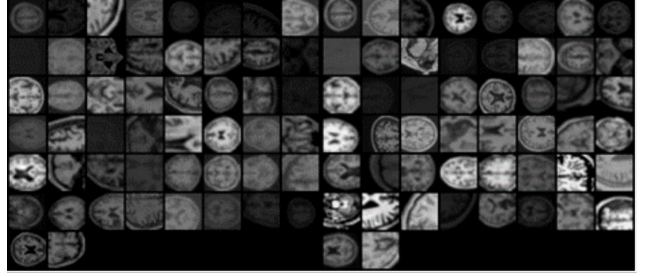


Figure 7. Different representations of the same image produced by SimCLR.

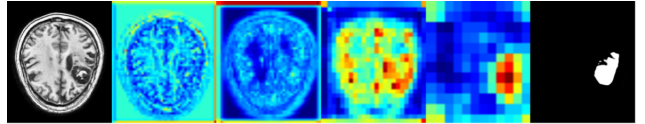


Figure 8. Feature visualization.

Model	Dice	MIoU	Precision
ResUNet	0.6810	0.5552	0.5583
ViT	0.6783	0.5496	0.5529
SimTrans	0.7585	0.6424	0.6453

Table 1. Segmentation results comparison.

the first stage, feature maps from the second stage, feature maps from the third stage, feature maps from the fourth stage, and the ground truth label map. From the visualization, it can be observed that the SimTrans model progressively increases its attention to the lesion regions, demonstrating its effectiveness in segmenting the target regions. The comparison results between SimTrans and two other networks, ResUNet [?]ResUNet) and ViT [2], are presented in Table 1.

It can be observed that when comparing SimTrans with ResUNet, there is an improvement of 0.0775 in Dice coefficient, 0.0872 in Mean Intersection over Union (MIoU), and 0.0870 in precision. These results indicate that the SimTrans network exhibits strong generalization ability and excellent segmentation performance. It can accurately segment the regions affected by brain stroke. The visualization of the segmentation results is shown in Figure 9. From left to right, each column represents the original image, the ground truth label map, the predicted map from ViT, the predicted map from ResUNet, and the predicted map from SimTrans.

The comparison of parameter count and computational complexity for each model is presented in Table 2. From the table, it can be observed that SimTrans has fewer parameters and lower computational com-

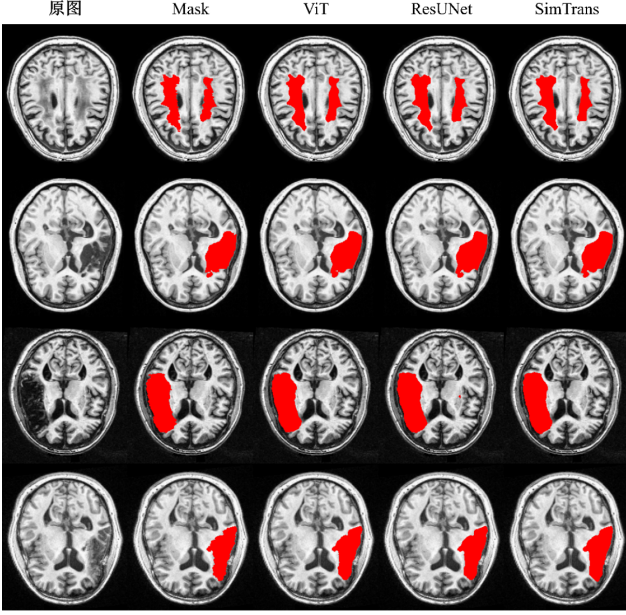


Figure 9. Model segmentation visualization.

Metric	ResUNet	ViT	SimTrans
Parameters/MB	24.01	108.25	87.32
Complexity/GMac	15.24	55.42	47.51

Table 2. Parameter and Computational Complexity comparison.

plexity compared to ViT, which is also a Transformer-based model. However, when compared to the classic ResUNet network model, which is based on ResNet as its backbone, there is still some gap. Although SimTrans shows improvement in accuracy, there is still room for progress in terms of model size and computational complexity.

5. Conclusion

This paper proposes an end-to-end self-supervised deep learning network model called SimTrans for the segmentation of brain stroke magnetic resonance imaging (MRI) images. SimTrans utilizes the self-supervised learning framework SimCLR to learn the data distribution and features from unlabeled data. The trained encoder framework, Swin Transformer, is then combined with a decoder structure for the segmentation of brain stroke regions. Additionally, a weighted structured loss function is introduced specifically for brain stroke segmentation to aid the model in achieving better segmentation results. Experimental results on the publicly available brain stroke dataset

ATLAS demonstrate the effectiveness of the proposed network model in brain stroke segmentation.

6. References

List and number all bibliographical references in 9-point Times, single-spaced, at the end of your paper. When referenced in the text, enclose the citation number in square brackets, for example [1]. Where appropriate, include page numbers and the name(s) of editors of referenced books. When you cite multiple papers at once, please make sure that you cite them in numerical order like this. If you use the template as advised, this will be taken care of automatically.

References

- [1] Ting Chen, Simon Kornblith, Mohammad Norouzi, and Geoffrey Hinton. A simple framework for contrastive learning of visual representations. In International conference on machine learning, pages 1597–1607. PMLR, 2020. 2
- [2] Alexey Dosovitskiy, Lucas Beyer, Alexander Kolesnikov, Dirk Weissenborn, Xiaohua Zhai, Thomas Unterthiner, Mostafa Dehghani, Matthias Minderer, Georg Heigold, Sylvain Gelly, et al. An image is worth 16x16 words: Transformers for image recognition at scale. arXiv preprint arXiv:2010.11929, 2020. 5
- [3] Sook-Lei Liew, Julia M Anglin, Nick W Banks, Matt Sondag, Kaori L Ito, Hosung Kim, Jennifer Chan, Joyce Ito, Connie Jung, Stephanie Lefebvre, et al. The anatomical tracings of lesions after stroke (atlas) dataset-release 1.1. bioRxiv, page 179614, 2017. 4
- [4] Ze Liu, Yutong Lin, Yue Cao, Han Hu, Yixuan Wei, Zheng Zhang, Stephen Lin, and Baining Guo. Swin transformer: Hierarchical vision transformer using shifted windows. In Proceedings of the IEEE/CVF international conference on computer vision, pages 10012–10022, 2021. 2
- [5] Fisher Yu and Vladlen Koltun. Multi-scale context aggregation by dilated convolutions. arXiv preprint arXiv:1511.07122, 2015. 3
- [6] Yulun Zhang, Kunpeng Li, Kai Li, Lichen Wang, Binyang Zhong, and Yun Fu. Image super-resolution using very deep residual channel attention networks. In Proceedings of the European conference on computer vision (ECCV), pages 286–301, 2018. 3